Imaging Coral I: Imaging Coral Habitats with the SeaBED AUV

Hanumant Singh[1]*, Roy Armstrong[2], Fernando Gilbes[2], Ryan Eustice[1], Chris Roman[1], Oscar Pizarro[1], and Juan Torres[2]

[1] Department of Applied Ocean Physics and Engineering, Woods Hole
 Oceanographic Institution, Woods Hole, MA 02543-1109, USA
[2] Department of Marine Sciences, University of Puerto Rico at Mayaguez,
 Mayaguez, PR 00681-9013, USA

The SeaBED autonomous underwater vehicle (AUV) is a new imaging platform designed for high resolution optical and acoustic sensing. This low cost vehicle has been specifically designed for use in waters up to 2000 m to carry out video transects, bathymetric and side-scan sonar surveys. In this paper we detail the systems issues associated with navigation, control, and imaging that led us to our particular hardware and software design choices so as to allow us to operate in shallow, shelf and ocean basin environments. We illustrate the strengths of our design with data obtained during two research cruises associated with mapping coral reefs off Puerto Rico and Bermuda. In both these cases, SeaBED was deployed in extremely challenging terrain associated off the shelf edge and was successful in returning high quality color imagery of deep coral habitats.

Key Words. AUV, coral, imaging, habitat.

1. Introduction

Affordable access to the seafloor for high-resolution imaging remains an elusive goal for researchers and users in the marine archaeology [1,2], marine biology [3,4], and marine geology and geophysics [5] communities. These disciplines all share a common need for high quality optical and acoustic surveys from small vessels of opportunity in depths extending just

*To whom all correspondence should be addressed. Phone: 508-289-3270; fax: 508-457-2191;
 e-mail: hanu@whoi.edu

beyond diver attainable depths to those associated with deep ocean basins. The navigation and control [6] and imaging [7] technologies associated with manned submersibles, remotely operated vehicles (ROVs) and towed vehicles that service such needs today, are expensive, require large ships and infrastructure, and are in short supply. The technologies associated with autonomous underwater vehicles (AUVs) are rapidly evolving to fill the requirements of these communities. A large number of AUVs are being designed, built and deployed in the support of such tasks. In the US there are a number of ongoing efforts, including commercial efforts such as those associated with the Bluefin Robotics AUVs [8] and the Remus AUVs [9] for oil and gas surveys and naval applications, the ABE AUV [10] designed for deep ocean scientific surveys, the Altex AUV [11] designed for under-ice surveys in the Arctic, and the Ocean Explorer and Morpheus AUVs [12] designed for coastal surveys. Other notable efforts abroad include the British Autosub AUV [13], the Norwegian Hugin AUV [14] and the Japanese Urashima AUV [15].

This paper outlines the design choices for the SeaBED AUV and lays out the results of our first set of test cruises aimed at characterizing deep water coral habitats. Section 2 goes over the vehicle components—imaging constraints driving our design, mechanical design, sensors, thruster design, power, and computing. Section 3 is dedicated to descriptions of the navigation and control systems. Section 4 describes our first science missions with Section 5 offering concluding remarks.

2. Basic Vehicle Components

2.1. Imaging Constraints

The fundamental issues associated with optical imaging as outlined above are the tradeoffs associated with vehicle speed, altitude and strobe recharge time as illustrated in Figure 1. For color imagery, for instance, it is imperative that the vehicle flies at altitudes between 3 and 4 m from the bottom. Also for photomosaicking and structure from motion applications the along track overlap must exceed 50%. Thus such a scenario, assuming a realistic strobe period of 2.75 sec, necessitates a working speed of 0.3 m/sec.

On the other end of the spectrum, at an altitude of 5 m, which is sufficient for black and white imagery, and an overlap of only 30%, which one might consider reasonable for photomosaicking in a flat area, the same strobe period of 2.75 sec yields a working speed of 0.9 m/sec.

These basic imaging constraints, as well as others detailed below, led us to design an AUV with controllable speeds between 0.2 and 1.2 m/sec with a capability of safely working close to the bottom. A requirement to
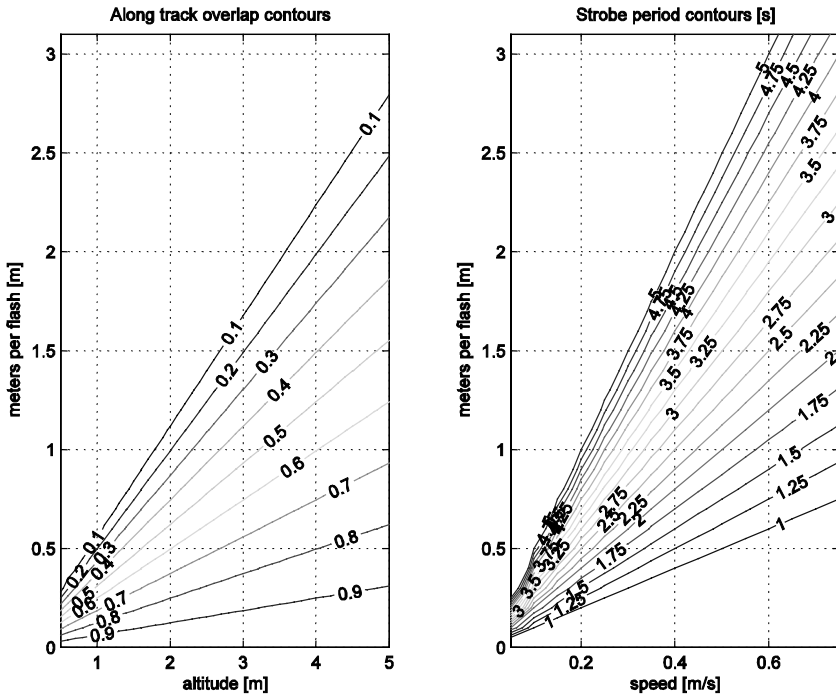
Figure 1. Vehicle speed–altitude–strobe-time characteristic curves.

build areal mosaics also led us to do require high navigation accuracies associated with side-to-side overlap.

2.2. Mechanical

The Seabed vehicle (Figs. 2 and 3) is composed of two torpedo-like body sections fixed to each other with vertical structural members. Each of the hull sections are 1.9 m long and 0.34 m in diameter. The separation between the hulls, centerline to centerline, is 1.1 m. The width of the vehicle, measured to the outside of the main thrusters, is 0.9 m. The overall weight of the vehicle is 200 kg. The internal parts of the vehicle are covered with ABS plastic skins to create the two torpedo shaped hulls.

The top hull of the vehicle contains the foam flotation and the main electronics housing which is also positively buoyant. The three main pressure housings on the vehicle – the electronics housing, the battery housing and the side scan sonar computer housing, are all constructed from 7075-T6 Al and have hemispherical end caps. Hemispherical end caps were chosen, in

Figure 2. The SeaBED AUV.

preference to flat endcaps, for the significant weight savings associated with such a design for housings over 15 cm in diameter. The foam flotation used is molded to shape and has a specific gravity of 0.4. The electronics in the main housing are connected to the other components by wet cabling routed through the vertical struts. The vertical struts have an airfoil profile and are oriented with the preferred direction of travel forward. Drag tests, detailed elsewhere [16] performed with a scale model indicated that the drag produced by the vertical airfoil shape was significantly less than the cylindrical shape originally envisioned. The main thrusters are also mounted with brackets made from airfoil shaped struts.

2.3. Sensors and Other Systems

The bottom hull of the vehicle contains all of the sensors. Most of the components in the bottom hull are negatively buoyant. The following list of sensors are currently integrated into the vehicle design.

- A high dynamic range digital still camera is the primary optical imaging sensor. This is a Pixelfly 1024×1280 12 bit CCD camera mounted in a flat glass plate housing. An example image using this
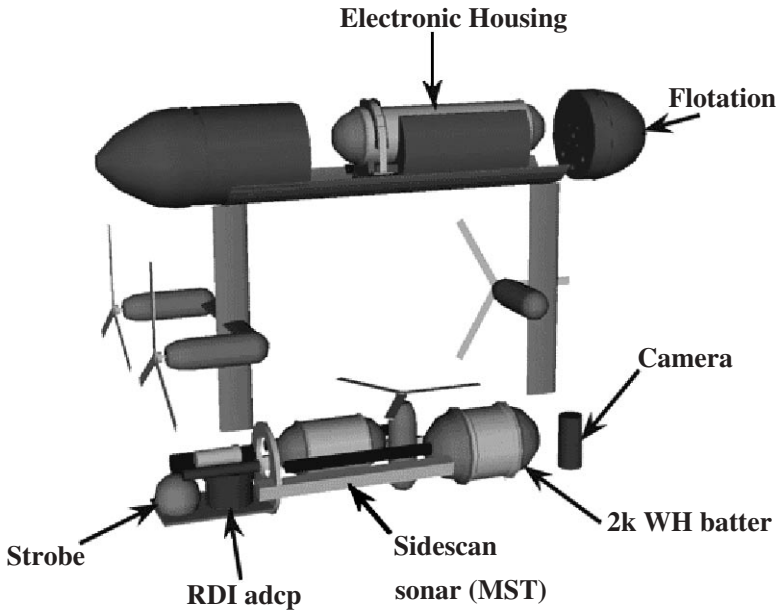
Figure 3. Vehicle CAD model showing the layout of the various sensors as well as the main mechanical components.

camera on SeaBED off Puerto Rico in a deep sea coral habitat is shown in Figure 4.

- A 300 kHz side scan sonar system (from Marine Sonics Technologies) with 6000 m rated transducers. This system operates on its own PC-104 stack running the Windows operating system. This system is controlled in its operation from the main vehicle computer system. Example data from this system in shallow water is shown in Figure 5.
- An RDI Workhorse Navigator 300 kHz ADCP is the primary navigation sensor and is operated in bottom lock mode. The ADCP provides measurements of velocity over the bottom, heading, altitude, pitch, roll, and integrated position. The doppler position estimate is accurate to 1–5% of the distance traveled.
- A 150 W-sec strobe is used for photographic illumination. The strobe is mounted 1.4 m aft of the camera to reduce the effects of lighting backscatter in the images.
- An Imagenex 881 scanning head pencil beam sonar is used to collect bathymetric data [CVIU]. The sonar frequency is variable between
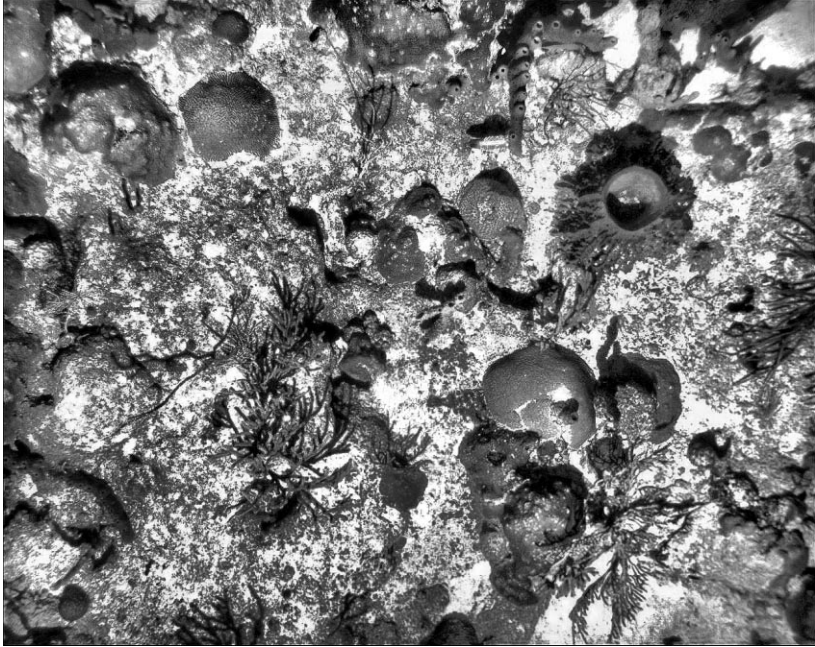
Figure 4. This image, taken with the SeaBED AUV, shows different species of corals, gorgonians, and sponges along the shelf edge off Puerto Rico.

300 kHz and 1.2 MHz. The sonar is mounted to scan athwartship and is capable of scanning ranges up to 200 m.

- A Paroscientific depth sensor provides depth information with an accuracy of centimeters.
- A Seabird conductivity and temperature sensor.
- An underwater acoustic modem is integrated in the vehicle to provide LBL support and low bandwidth communication with the surface. At present, the modem is programmed to send 32 byte data packets back from the vehicle and listen for abort commands sent from the surface to the vehicle while it is operating.
- An Ascent/Descent weight system is used to help the vehicle transit to the bottom and provide a factor of safety for the vehicle ballasting. Typically the vehicle is ballasted one pound buoyant to allow the vehicle to float up to the surface in case of a system emergency.
- A Crossbow Inertial Measurement Unit that is mounted inside the main electronics housing and consists of angular gyroscopic rate sensors, accelerometers and a fluxgate compass.
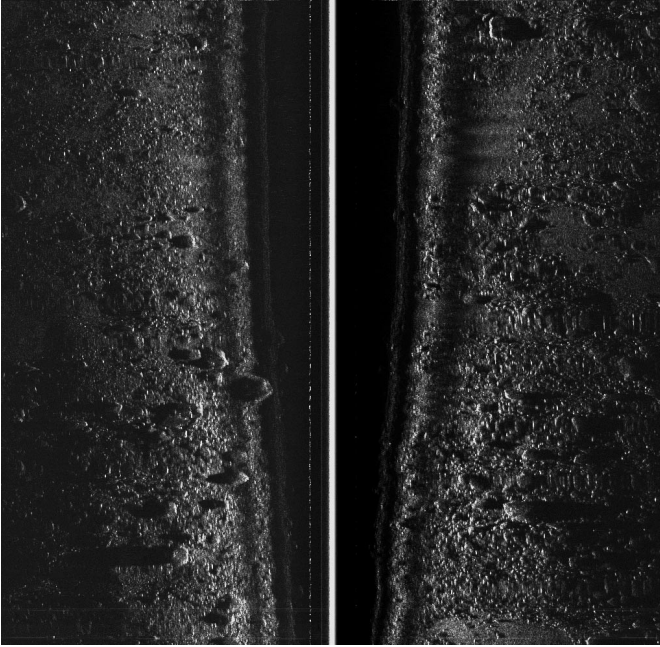
Figure 5. Side scan sonar data obtained with the SeaBED AUV. The site is off Woods Hole, MA and was used as a bombing range towards the end of the Second World War.

- Tracking and Emergency. The vehicle carries an acoustic ultra-short baseline tracking beacon (from ORE corporation) to provide range and bearing at a top side display. This information is used only to provide an approximate location of the vehicle during a mission. An emergency strobe and emergency RF tracking beacon are used at all times to help aid in the recovery of the vehicle.

2.4. Thrusters

The four thrusters used to propel the vehicle are identical DC brushed motors enclosed in one atmosphere pressure housings. The housings use a magnetic coupling between the motor and the shaft for the propeller, avoiding the need for high pressure shaft seals which typically have high levels of friction. The motors turn 24″ diameter graphite propellers with 12″ of pitch.

The thruster motors are torque controlled using a PWM switching controller. Operating in open loop, a specified motor current will result in a corresponding vehicle velocity through the water in a steady state situation.

In closed loop control, the desired motor current is manipulated to achieve a desired vehicle speed over ground. Vehicle speed is measured with a doppler velocity log. A simple relationship between thruster motor current and the actual thrust produced was determined using a Bollard type test with a calibrated load cell [16]. Using these motors and propellers we have been able to control the vehicle to do survey work at speeds between 0 and 1 m/sec. In general, accurately controlling slower vehicle speed is more difficult given the complex relation between thruster motor current and the actual thrust produced around the zero operating point.

2.5. Power

The vehicle carries a compact 2 kWh battery pack. The pack consists of 126 high-energy density Li-ion secondary D cells (from Eagle Pitcher Corporation) and the necessary circuitry for monitoring and recharging these cells without venting the battery housing. The battery pack is organized in 14 serial stacks. Each individual stack is made up of nine cells connected in parallel. The monitoring circuitry provides real-time voltage and charge capacity measurements for our battery pack.

The main vehicle power varies between 56 and 42 V and is fed to a number of high input range DC–DC converters that convert this voltage to the appropriate bus voltages (5, 12, 24, and 48 V) required for the computing resources, sensors and thrusters. With a typical sensor load this pack allows us to run for eight hours.

We have taken pains to provide separate isolated power supplies to prevent electrical noise from corrupting different sensors. While this may be considered wasteful, as the individual converters have power losses associated with efficiency (even considering in our case that we turn them off with relays if they are not required) the payoff lies in our ability to seamlessly integrate a large variety of sensors. For example, the sidescan sonar and the ADCP both operate at 300 kHz. However, they do not interfere with each other and the fact that we can run them asynchronously is a testament to the isolation that we have achieved through our power bus design.

2.6. Computing

The main computing source on the vehicle is a PC-104 166 MHz Pentium system running Redhat Linux 6-2. The Linux operating system has proved a stable basis for the operation of the AUV as well as been a boon for software development.

The vehicle control loop runs at 10 Hz. The basic software architecture follows a multi threaded approach, with individual threads designated

for hotel management, control execution, sensor support, data logging and mission command. Operation of the vehicle consists of a main program to take care of sensors, hotel, logging and control running in parallel with a mission planning program which governs the higher level task execution specific to a given mission. Missions are defined in a mission script format consisting of a sequence of behavior specific tasks and related hotel information. The mission planning program (written in Perl) communicates with the main program through a socket connection by sending formatted messages. This split between a mission planner and main routine has helped separate the higher and lower level tasks of vehicle operation. The messages sent by the mission planner are composed of lower level goals that keep the main software separated from detailed task specific support.

Vehicle data is logged during operation to ASCII formatted files that are organized by date and mission name. The core navigation data is logged at 5 Hz. The camera images generate the most significant amount of data. At the maximum rate of an image every 2.5 sec, determined by the speed images can be written to the hard drive and the charging time required by the strobe, the camera generates ~ 1 MB/sec. The sidescan sonar data is stored on the PC-104 computer dedicated to the sidescan system.

3. Navigation and Dynamics

3.1. Vehicle Shape

The SeaBED vehicle is shaped to create a passively stable platform in roll and pitch. The separation of the two torpedo shaped hulls, the top containing syntactic foam flotation and the bottom containing heavy components, has many advantages for an imaging platform. The vehicle is very stiff in roll and pitch while still easily controlled in the four other degrees of freedom. This separation also minimizes the effects of body lift and body roll which are associated with single hull torpedo style AUVs. This configuration also helps decouple the other controllable axes, making control design and development a simpler task. The theoretical estimate for the metacentric height, the separation between the CG (center of gravity) and CB (center of bouyancy) is approximately 23 cm. This value for metacentric height is significantly more than the typical 2–5 cm separations associated with most torpedo shaped vehicles.

Typical pitch and roll excursion for the vehicle, when excited by its own thrusters, are less than two degrees and often less than one degree in steady state situations. This behavior is illustrated in Figure 6, which shows approximately 10 min of pitch and roll data during a typical survey over a relatively flat bottom. The roll motion is slightly excited as the vehicle
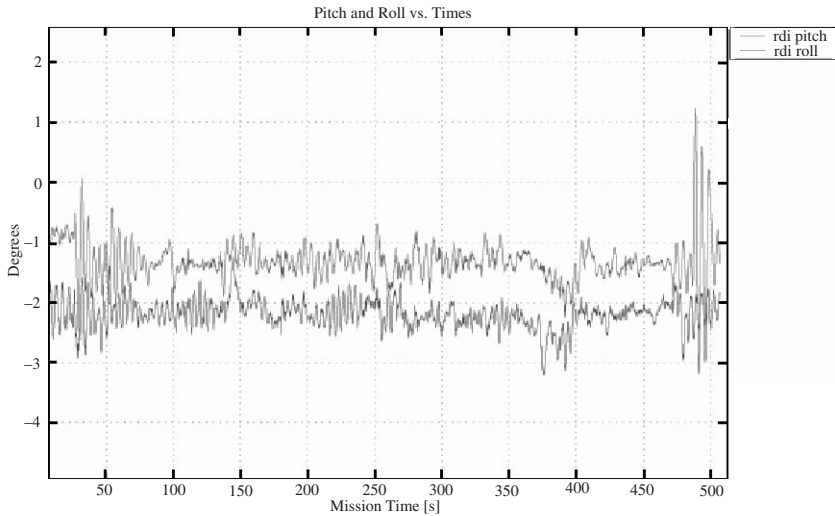
Figure 6. Pitch and roll for a typical mission profile. The large metacentric height of the vehicle makes SeaBED a very stable platform.

descends to depth. The pitch and roll natural frequencies for the vehicle are both approximately 0.3 Hz.

3.2. Control System

The basic control architecture is set up similarly for each controlled axis, heading, speed and depth. These axes are then controlled independently with individual servos. In each case the servos are setup to handle goal and reference states. The goal states are manipulated at the level of a desired vehicle behavior. An example would be flying the vehicle at a desired (goal) altitude. The goal states are then filtered with a simple model of the vehicle dynamic response to create a reference trajectory that is achievable by the vehicle. The reference state is then fed to the axis servo controller.

Shaping the reference trajectory with an approximate vehicle response is a simple way of avoiding actuator saturation, typical of commanding references that the vehicle cannot achieve. Also, this decoupling of goal and reference make the transition between different modes of controller operation seamless, such as the transition between flying at a fixed depth and flying to maintain a specified altitude above the bottom. The large majority of control computation involves the creation of servo references from desired goals. The reference trajectory generation is decoupled into a depth servo and

heading and speed servos. The depth trajectory uses the desired goal, depth measurement and altitude measurement to generate a depth reference.

The heading and speed trajectories are more complicated as they may be coupled. The vehicle behaviors in the XY plane consist of three basic types; goto a point (x, y), goto a point (x, y) along a line and goto a point (x, y) along a line while maintaining a specific heading. In the first case, the heading and speed trajectories are decoupled and the vehicle motion is subject to water current disturbances. In a typical situation the vehicle will trace out a curved "fishhook" path as it approaches the desired end point. The second situation requires the trajectory generation to account for the presence of a current disturbance. In this case we use a vector field, which surrounds the desired trackline, to generate the desired vehicle velocity that will keep the vehicle traveling along the line. With the desired vehicle velocity defined by the vector field, the heading and speed trajectories are defined to produce this desired velocity. The heading trajectory uses the current heading and velocity to produce a reference heading which accounts for a current disturbance.

Control of each servo is done with decoupled PID controllers with additional feedforward terms. In each case the servo controllers generate a desired thrust which is then sent to individual thruster control loops for each of the four thrusters. The thruster control loop manipulates the motor voltage to achieve a desired thrust, which can be related to the motor current. The thruster control loops run at 100 Hz and are tuned to achieve a desired motor current in approximately 0.1 sec.

Results from an example survey pattern are shown in Figures 7 and 8. The vehicle was commanded to execute two parallel tracklines spaced 1 m apart while maintaining a constant altitude. The plots show that the vehicle can easily maintain depth and XY position of the order of ~10 cm.

4. A Shelf Edge Transect off Southwestern Puerto Rico

The first non-local deployment of the SeaBED AUV was in Puerto Rico. During March of 2002, we used the SeaBED for characterizing the shelf edge and the deep coral reef zones of the insular slope off southwestern Puerto Rico. While numerous assessments of coral reef habitat have been conducted throughout the Caribbean islands and elsewhere using SCUBA, there is limited information on the deeper reefs zones that lie beyond the range of safe diving operations.

An evaluation of deep-water fish habitats and abundance around Puerto Rico and the US Virgin Islands, at depths ranging from 36 to 758 m, was conducted aboard the Johnson Sea-Link II submersible [17]. In Jamaica, the deep fore reef slope off Discovery Bay was described to depths of 305 m
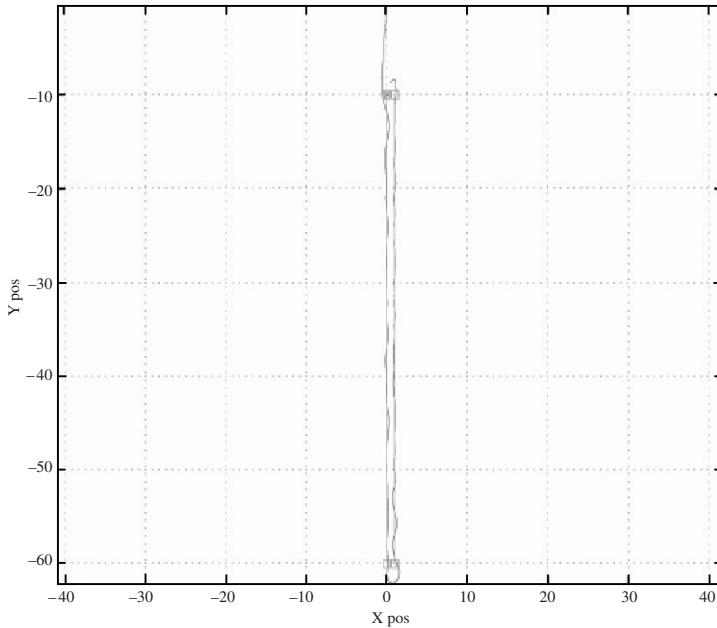
Figure 7. The XY plot for a survey mission consisting of two parallel tracklines spaced one meter apart. The vehicle can achieve such commanded trajectories accurate to a few cm.

using the Nekton Gamma submersible [18]. In the deeper coral reef zones, the *in-situ* digital imagery obtained by submersibles and AUV's provide the only source of information to characterize and map these benthic habitats.

    We used the 42′ R/V Sultana from the University of Puerto Rico's Department of Marine Sciences as shown in Figure 9 as a support vessel. The main purpose of this deployment was to perform engineering tests of the vehicle and to build initial photomosaics of shallow-water coral reefs sites. We also included one deep transect along the insular slope south of La Parguera starting at 20 m over the shelf edge to 125 m depth as shown in Figure 10.

    We followed this track line at an altitude of 3–4 m from the bottom to allow the identification of individual coral species. What made this task challenging was the steep, 75° slope of this transect (Fig. 11). At such high angles and low altitudes off the bottom the placement of the altitude sensor is crucial since it defines altitude with respect to the vehicle. Under these conditions we obtained 30–40% overlap in the digital still camera imagery, which included co-registered bathymetry. A total of 200 photographs were obtained. The digital photos were enhanced with standard image processing tools and the
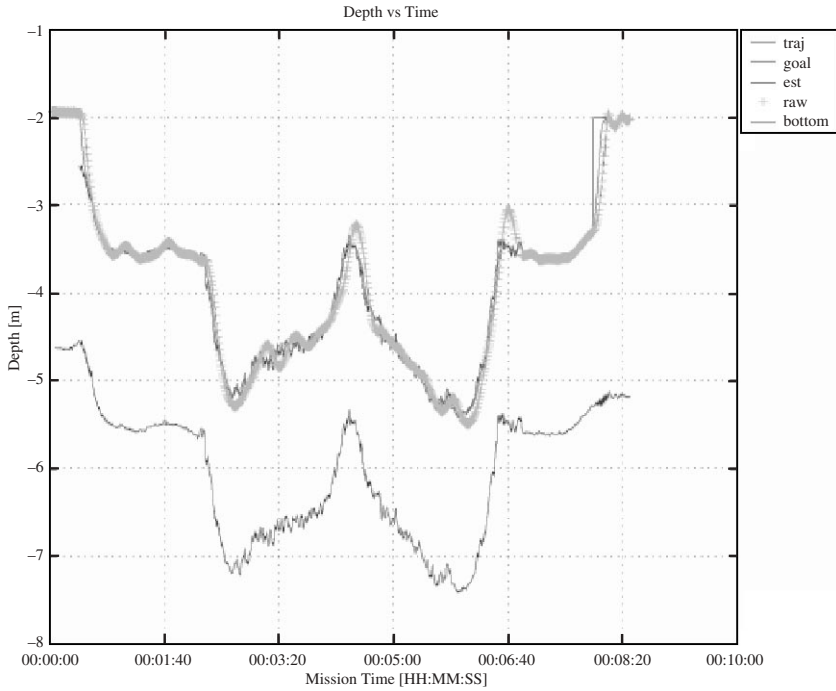
Figure 8. The depth plot for a typical survey mission shows that the vehicle can easily follow the bottom at a fixed altitude within a few cm.

Figure 9. The Department of Marine Sciences 42′ R/V Sultana with the AUV lashed to the stern.
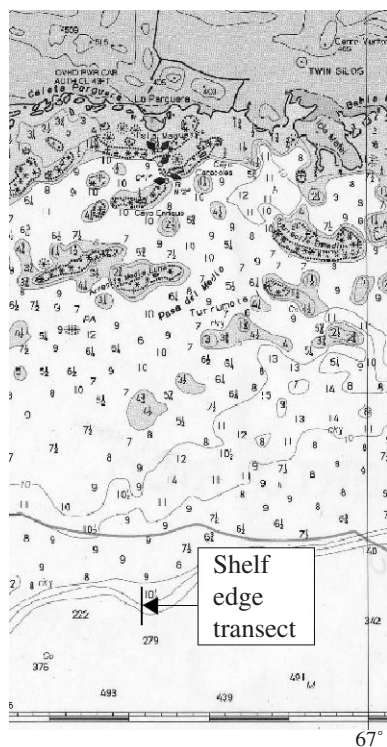
Figure 10. Map of La Parguera, southwestern Puerto Rico, with the position of the shelf edge transect. Soundings are in fathoms.

individual coral colonies were screen digitized for calculating the percent coral cover from each photograph.

4.1. Benthic Description

Six distinct benthic zones could be identified from the insular shelf transect photography as plotted in Figure 12. The shelf edge reef at 24–30 m had the highest coral cover (mean = 25%). In this zone the dominant coral species is *Montastraea annularis*. Scattered colonies of *Agaricia* sp., *Diploria* sp., and *Porites astreoides* are also present. Some sponges and octocorals can also be seen in the photograph (Fig. 13). The remaining bottom surface is dominated by fleshy algae, sand, coral debris, and calcareous algae (e.g. *Halimeda opuntia*). Sponges are the dominant macro invertebrate at intermediate zones (40–90 m). The deeper insular slope at 95 m depth is a hard
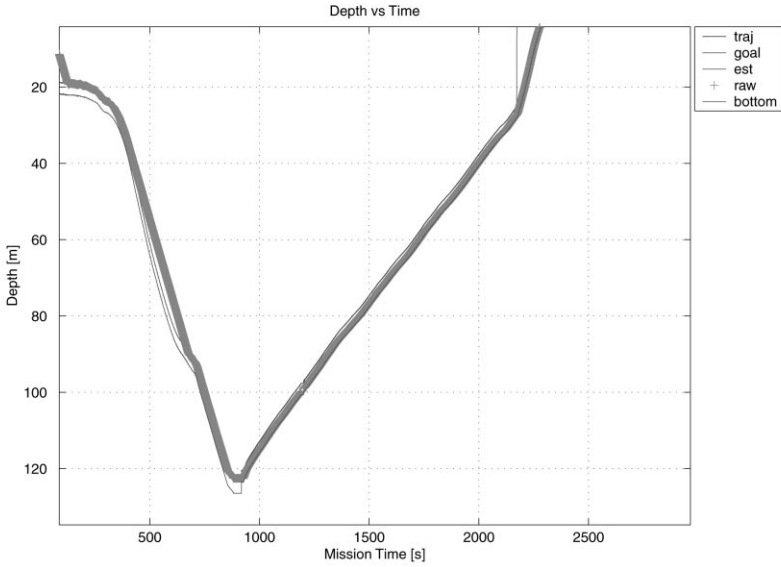
Figure 11. Depth plot for entire transect. We followed the sharp slope at an altitude of 3–4 m.
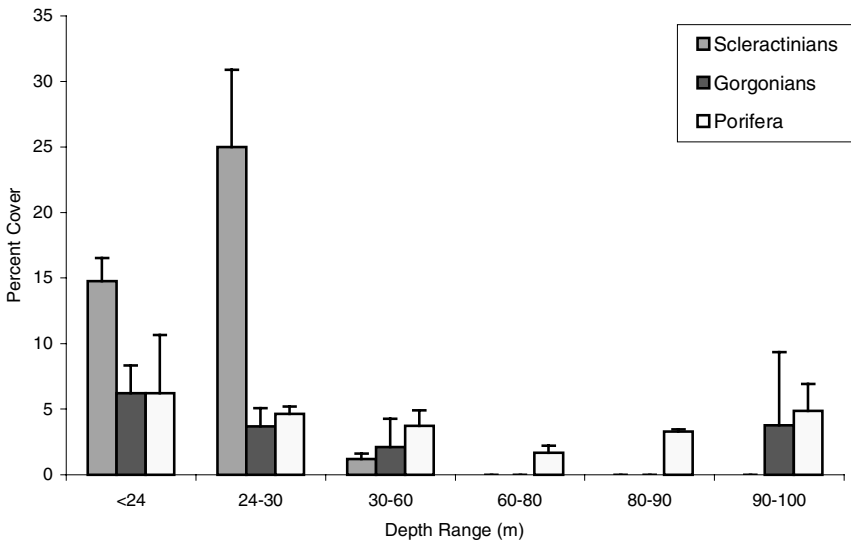

Figure 12. Percent cover of corals, gorgonians and sponges for each distinct benthic zone.
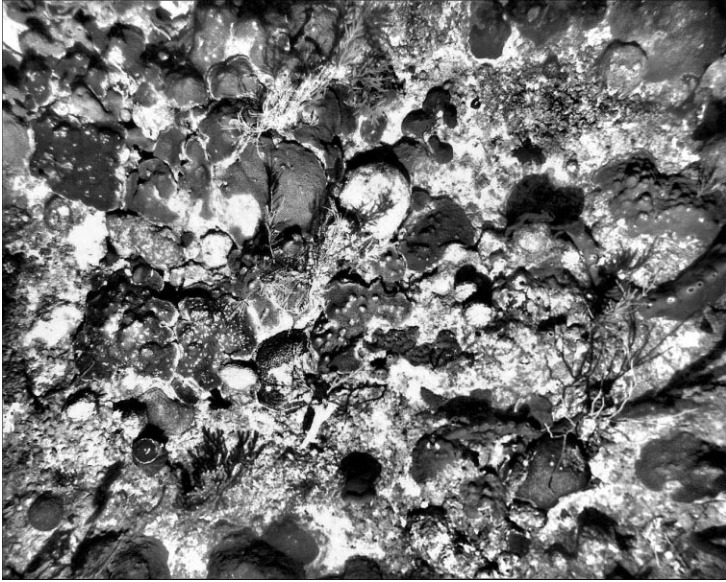
Figure 13. At the shelf edge (24 m depth) the dominant coral species are *Montastraea annularis* along with scattered colonies of *Agaricia* sp., *Diploria* sp., and *Porites astreoides.* Coral cover in this photograph is estimated at 30.2%.

ground covered by calcareous algae and sclerosponges (Fig. 14). Black corals (class: Anthozoa, order: Antipatharia), possibly the genus *Cirrhipathes* (sea whips) and a distinctive big colony of the species *Antipathes gracilis* (class: Anthozoa, order: Gorgonacea) are also present in this photograph.

In some cases the identification of corals and other benthic organisms from the photography was difficult due to the large, up to 4 m distance between the camera lens and the substrate. The high slope of this transect presented another challenge. In spite of these difficulties, a continuous, high quality photo transect of the deep shelf edge reef was obtained. In other shelf edge areas with more gentle (45°) slopes, the camera to substrate distance could be reduced significantly facilitating the identification of corals and other reef organisms to the species level.

5. Conclusions

In this paper we have outlined the constraints and design decisions that went into building the SeaBED AUV and have presented the brief results of our first test cruise associated with mapping coral habitats off of Puerto Rico.

Figure 14. The insular slope at 95 m depth is a hard ground covered by calcareous algae and sclerosponges. A distinctive big colony of the deep-water gorgonian *Antipathes gracilis* can be seen near the upper left corner.

The SeaBED AUV provided new information on a little known coral reef habitat that is common along the upper insular slopes of many Caribbean Islands. An unprecedented digital camera transect provided data on zonation patterns, species composition and abundance, and geomorphological features of the insular shelf slope off southwestern Puerto Rico.

We now expect to transition the SeaBED AUV from a developmental stage to an operational vehicle available for conducting surveys for a variety of users in diverse applications.

References

1. Ballard, R.D., McCann, A.M., *et al.*, 2002, The discovery of ancient history in the deep sea using advanced deep submergence technology: Deep Sea Res., v. 1, no. 47, p. 1591–1620.

2. Ballard, R.D., Stager, L.E., *et al.*, 2002, Iron age shipwrecks in deep water off Ashkelon: Israel Am. J. Archaeol., v. 106, no. 2.

3. Greene, G.H., Yoklavich, V.M., *et al.*, 2000, Mapping and classification of deep seafloor habitats: ICES 2000 Annual Science Conf., Belgium.

4. Gordon, D.C., Kenchington, E.L.R., *et al.*, 2000, Canadian imaging and sampling technology for studying marine benthic habitat and biological communities: ICES 2000 Annual Science Conf., Belgium.

5. Shank, T., Hammond, S., *et al.*, 2002, Time-series exploration and biological, geological, and geochemical characterization of the rosebud and calyfield hydrothermal vent fields at 86°W and 89.5°W on the Galapagos Rift: EOS Trans. AGU, v. 83, no. 47, Fall Meeting.

6. Whitcomb, L.L., Yoerger, D.R., *et al.*, 2000, Advances in underwater robot vehicles for deep ocean exploration: navigation, control and survery operations: Proc. 9th Int. Symp. on Robotics Research, Springer, London.

7. Singh, H., Adams, J., *et al.*, 2000, Imaging underwater for archeology: Am. J. Field Archaeol., v. 27, no. 3, p. 319–328, Fall.

8. http://www.bluefinrobotics.com

9. http://www.hydroidinc.com

10. Yoerger, D.R., Bradley, A., Walden, B., Singh, H., and Bachmayer, R., 1998, Surveying a subsea lava flow using the autonomous benthic explorer (ABE): Int. J. Systems Sci., v. 29, no. 10, p. 1031–1044.

11. http://www.mbari.org/education/cruises/Altex/

12. Smith, S.M., An, P.E., Holappa, K., *et al.*, 2001, Morpheus: ultra modular AUV for coastal survey and reconnaissance: IEEE Trans. Oceanic Eng., v. 26, no. 4, p. 453–465.

13. Babb, R.J., 1993, Scientific surveys in the deep ocean using AUV's: the Autosub project: Proc. AUV 1993 Conf., Washington, DC.

14. Jalving, B., 1994, The NDRE-AUV flight control system: IEEE J. Oceanic Eng., v. 19, no. 4, p. 497–501.

15. Urashima, K.T., Aoki, T., Tsukioka, S., Murashima, T., Nakajoh, H., and Fujita, T., 2000, The development of the deep sea cruising AUV: Proc. UT2000 Conf., Tokyo, Japan.

16. Roman, C., Pizarro, O., Eustice, R., and Singh, H., 2000, A new autonomous underwater vehicle for imaging research: Proc. 2000 MTS/IEEE Oceans Conf., Providence, RI, v. 1, p. 153–156.

17. Nelson, W.R. and Appeldoorn, D.S., 1985, A submersible survey of the continental slope of Puerto Rico and the U.S. Virgin Islands, Cruise Report, R/V Seward Johnson, October 1–23, 76pp.

18. Land, L.S. and Moore, C.H., 1977, Deep forereef and upper island slope, North Jamaica, in Frost, S., Weiss, M., and Saunders, J., eds., Reef and Related carbonates—Ecology and Sedimentology, Studies in Geology No. 4, American Association of Petroleum Geologists, p. 53–65.